

PCCP

Accepted Manuscript



This is an *Accepted Manuscript*, which has been through the Royal Society of Chemistry peer review process and has been accepted for publication.

Accepted Manuscripts are published online shortly after acceptance, before technical editing, formatting and proof reading. Using this free service, authors can make their results available to the community, in citable form, before we publish the edited article. We will replace this *Accepted Manuscript* with the edited and formatted *Advance Article* as soon as it is available.

You can find more information about *Accepted Manuscripts* in the [Information for Authors](#).

Please note that technical editing may introduce minor changes to the text and/or graphics, which may alter content. The journal's standard [Terms & Conditions](#) and the [Ethical guidelines](#) still apply. In no event shall the Royal Society of Chemistry be held responsible for any errors or omissions in this *Accepted Manuscript* or any consequences arising from the use of any information it contains.

Remarkable Effects of Solvent and Substitution on Photo-dynamics of Cytosine: A Femtosecond Broadband Time-resolved Fluorescence and Transient Absorption Study

Chensheng Ma,*¹ Chopen Chan-Wut Cheng,² Chris Tsz-Leung Chan,² Ruth Chau-Ting Chan² and Wai-Ming Kwok*²

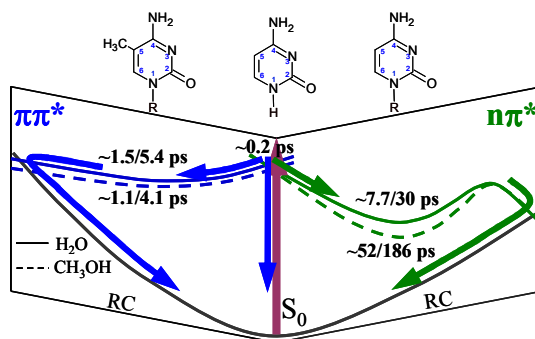
¹ College of Chemistry and Chemical Engineering, Shenzhen University, Shenzheng, Guangdong, P. R. China.

² Department of Applied Biology and Chemical Technology, The Hong Kong Polytechnic University, Hung Hom, Kowloon, Hong Kong, P. R. China.

E-mail: macs@szu.edu.cn; wm.kwok@polyu.edu.hk

Table of Content Graphic

Solvent alters differently rate of $\pi\pi^*$ and $n\pi^*$ decay while substitution enhances or eliminates the $n\pi^*$ from cytosine nonradiative deactivation.



ABSTRACT. Cytosine (Cyt) among all the nucleic acid bases features the most complex and least understood nonradiative deactivation, a process that is crucially important to its photostability. Herein, the excited state dynamics of Cyt and a series of its N1- and C5-derivatives, including the full set of Cyt nucleosides and nucleotides in DNA and RNA and the nucleosides of 5-methyl cytosine the 5-methylcytidine and 2'-deoxy-5-methylcytidine, have been investigated in water and in methanol employing femtosecond broadband time-resolved fluorescence coupled with fs transient absorption spectroscopy. The results reveal remarkable state-specific effects of the substitution and solvent in tuning distinctively the timescales and pathways of the nonradiative decays. For Cyt and the N1-derivatives, the nonradiative deactivations occur in a common two-state process through three channels, two from the light-absorbing $\pi\pi^*$ state with respectively sub-picosecond (~ 0.2 ps) and picosecond (~ 1.5 ps) time constant, and the third is due to an optically dark $n\pi^*$ state with lifetime ranging from several to hundreds picoseconds depending on solvent and substitutions. Comparing to Cyt, the presence of the ribose or deoxyribose moiety at the N1 position of N1-derivatives facilitates formation of the $n\pi^*$ at the sub-picosecond timescale and at the same time increases its lifetime by ~ 4 — 6 times in both water and methanol. In sharp contrast, the existence of the methyl group at C5 position of the C5-derivatives eliminates completely the sub-picosecond $\pi\pi^*$ channel and the channel due to the $n\pi^*$, but on the other hand slows down the decay of $\pi\pi^*$ state which after relaxation exhibits a single time constant of ~ 4.1 to ~ 7.6 ps depending on solvent. Varying solvent from water to methanol accelerates only slightly the decay of $\pi\pi^*$ state in all the compounds; while for Cyt and its N1-derivatives, this change of solvent also retards strongly the $n\pi^*$ channel, prolongs its lifetime from such as ~ 7.7 ps in water to ~ 52 ps in methanol for Cyt and from ~ 30 ps in water to ~ 186 ps in methanol for deoxycytidine. The spectral signatures we obtained for the $\pi\pi^*$ and $n\pi^*$ state allow unambiguous evidence for clarifying uncertainties on the excited states of Cyt and the derivatives. The results provide

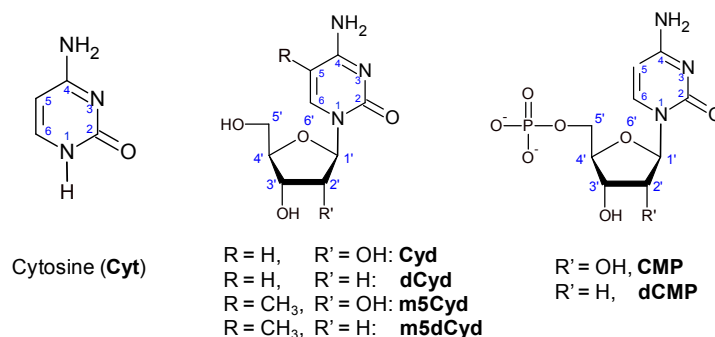
a unifying experimental characterization in an improved level of detail about the photophysics of Cyt and its analogues in biologically relevant conditions and may help understanding the photostability as well as photo-damages of the bases and related DNAs.

INTRODUCTION

All naturally occurring nucleobases, upon UV excitation, have ultrafast decay routes in sub-ps timescale from light-absorbing $\pi\pi^*$ state to the ground (S_0) state.^[1,2] The ultrafast decays arising from the highly efficient internal conversion are often invoked as the principal mechanism against photo-damage and also regarded the main source of the bases being selected as the building blocks of genetic materials.^[1-4] A growing number of recent studies show, however, that the sub-ps decay of $\pi\pi^*$ may contribute only partially to the overall nonradiative dynamics, other processes taking place on slower timescales through the $\pi\pi^*$ or more importantly through optically dark state such as of $n\pi^*$ in parentage may play a significant role.^[1-5] The complexity is rooted in the intrinsic property of the bases in having peculiar topology of the $\pi\pi^*$ potential energy surface (PES) and low lying $n\pi^*$ states that may couple nonadiabatically with both the $\pi\pi^*$ and S_0 . However, owing to the short lifetimes and complex dynamics that may vary from subtle changes in factors such as substitution and medium condition, to directly probe the $\pi\pi^*$ and at the same time to resolve the $n\pi^*$ state has remained a challenging task. As a consequence, despite the invaluable insights led by the extensive studies, there are still important questions to answer, including such as whether for a particular base there is indeed a participation of $n\pi^*$ state in the decay process,^[1-9] the precise timescales, pathways, and extents to which the $n\pi^*$ competes with $\pi\pi^*$, and how these are affected by environmental factor and covalent modification of the bases.^[2-5]

With very few exceptions,^[1c,4d,4f,5,6i,8a-b] most of the previous studies on the nucleobases in solution were performed in water.^[1] In DNA and RNA, the bases are however subject to an interior solvation environments that are much less polar and with hydrogen (H)—bonding configurations different than in water.^[1a,1b] Also, the bases exist with substitution of certain hydrogen atom by ribose (in RNA) or deoxyribose (in DNA) and with some other hydrogen substituted by such as the methyl group for the case of

minor bases. To elucidate the effects of solvent and the substitution on the excited state dynamics is therefore not only crucial for a fuller description of the bases in their monomeric form but is also a prerequisite for understanding the photophysics of DNA and RNA assemblies. Herein, as a case study, we present a direct probe of the full deactivation cascades for cytosine (Cyt) and a series of its N1- and C5-substituted derivatives (Scheme 1) in solvents of different polarity and H-bonding capacity.



Scheme 1 Cytosine and its N1 and C5 derivatives studied.

As the only common pyrimidine base between DNA and RNA, Cyt is known for its particularly complex excited state structure^[2-4,6-11] which might allow for parallel operation of multiple decay paths from $\pi\pi^*$ and $n\pi^*$ states.^[6,7,9-11] The excited state dynamics reported for Cyt are, however, varied depending on the conditions and methods used for the measurements. In water, Cyt and its N1 derivatives including some of its nucleosides and nucleotides were reported to display very rapid decay from the light-absorbing $\pi\pi^*$ state. The decay of $\pi\pi^*$ was respectively described to be single exponential (with time constant of ~ 1.0 ps) and bi-exponential (with ~ 0.2 and ~ 1.3 ps time constants) by the fs transient absorption (fs-TA)^[1a,2a] and fs fluorescence up-conversion (fs-FU) measurement.^[4a,4b] In addition to the $\pi\pi^*$ state, a longer-lived species (~ 33 - 39 ps lifetime) attributed to a dark $n\pi^*$ state was reported for the N1-derivatives dCyd, CMP, and dCMP in water.^[2c,3] Whether the $n\pi^*$ is present for the parent molecule Cyt is

however a controversial issue. Whilst an earlier fs-TA study based on probe of excited state dynamics at selected absorption wavelengths reported an involvement of the $n\pi^*$,^[2c] more recent ps time-resolved infrared (ps-TRIR) work stressed an absence of the $n\pi^*$ in Cyt.^[3] On the other hand, ultrafast studies on Cyt in the gas phase reported decay dynamics described by time constants of tens fs to several ps^[12] with the $n\pi^*$ state playing an important role as suggested by a number of sophisticated theoretical computations.^[6-11] There is however to the best of our knowledge no time-resolved study on Cyt and any of the derivatives (Scheme 1) in solvent other than water.

The C5 derivatives we investigated (m5Cyd and m5dCyd, Scheme 1) are the nucleosides of 5-methyl cytosine (m5Cyt), a minor base from DNA methylation which is known for its role as the mutational hotspot in skin tumours.^[13] Ultrafast studies on m5Cyd and m5dCyd in water reported transient species with $\sim 6\text{--}7$ ps lifetime^[2b,4c] showing complex fluorescence decay.^[4c] The cause of the complexity and influence of C5 substitution on the decay dynamics, especially those related to the $n\pi^*$ state, have so far remained elusive.

The uncertainties and the different dynamics reported for Cyt in water *vs* in the gas phase and between Cyt and its N1 and C5 derivatives raise questions about (i) the detailed pathway of $\pi\pi^*$, (ii) the role of $n\pi^*$, and (iii) influences of solvent and N1- and C5-substitution on the nonradiative decays. To help address all these questions, we have performed an integrated spectroscopic investigation which we combined steady state measurements with fs broadband time-resolved fluorescence (fs-TRF), fluorescence anisotropy (fs-TRFA), and transient absorption (fs-TA) on Cyt and all the derivatives in Scheme 1. The study was done in water and for comparison in a less polar protic solvent methanol in order to assess effect of solvent on the dynamics and pathways of the nonradiative deactivation. Featuring simultaneously the wavelength resolution and fs time resolution, our fs broadband spectroscopy provides an important complement to the

literature fs-TA,^[2] fs-FU,^[4] and ps-TRIR^[3] methods which are lack of either the spectral resolution or the time resolution in fs domain. The wavelength resolution of our method allows producing spectral signature for extremely short-lived species,^[5c,14,15] a feature crucial for identifying explicitly the $\pi\pi^*$ and $n\pi^*$ state in the deactivation of Cyt and the derivatives. Besides, with the fs-TRF to probe the bright $\pi\pi^*$ state and the fs-TA to monitor in addition the optically dark $n\pi^*$ state as well as the recovery and relaxation of the S_0 , the integration of fs-TRF and fs-TA makes possible to determine not only the dynamics of excited state decays but also the correlations in dynamics between the decays and S_0 recovery which enable to unveil the overall cascade of the deactivation processes. The results we obtained provide direct evidence for clarifying the uncertainty on the Cyt deactivation and show unprecedented effects of solvent and the N1- and C5-substitution in modulating distinctively dynamic competition between the $\pi\pi^*$ and $n\pi^*$ for nonradiative decays that occur in largely varied timescales from sub-ps to hundreds ps after the excitation.

RESULTS

Steady state spectroscopy

Figure 1 displays steady state absorption and fluorescence spectra recorded for Cyt, the N1 derivatives Cyd and dCyd, and the C5-derivatives m5Cyd and m5dCyd in water and methanol. Comparison of the spectra in water for Cyt and all of the N1-derivatives (including CMP and dCMP) is presented in Figure S1 in the supporting information (SI). Due to the low solubility, no spectra (both in the steady state and fs time-resolved measurements) were obtained for CMP and dCMP in methanol. Key spectral parameters including such as the wavelengths of maximum absorption and fluorescence spectra, the maximum molar absorption coefficients and fluorescence quantum yields for all the

systems examined are compiled in Table 1. For compounds that were studied previously in water, the results we obtained from the steady state measurement are consistent with those in the literature.^[2b,4a-c]

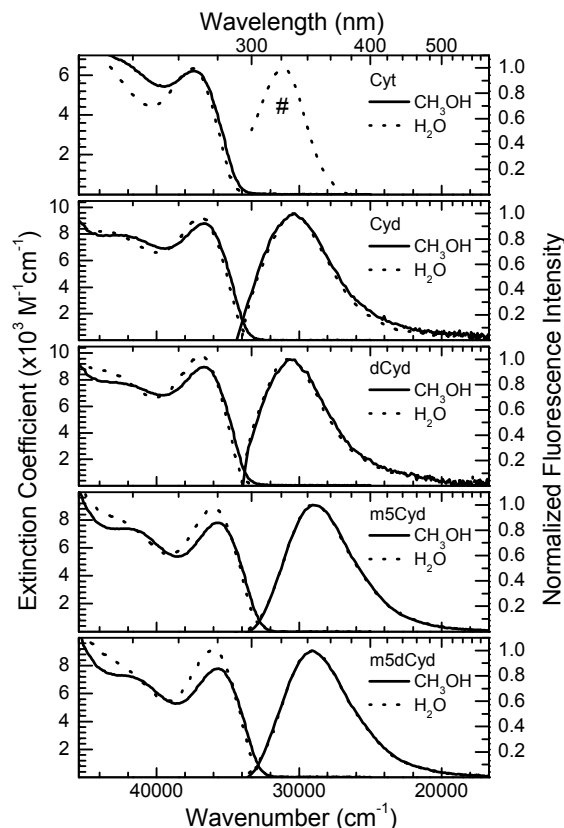


Figure 1. (Left) steady state absorption and (right) normalized fluorescence spectra ($\lambda_{\text{exc}} = 267 \text{ nm}$) recorded for Cyt, Cyd, dCyd, m5Cyd, and m5dCyd in water (dotted lines) and in methanol (solid lines). #From [16a].

It can be seen from Figure 1 and Table 1 that varying solvent from methanol to water affects only subtly the steady state spectra, leading to such as small wavelength blue-shifts (by $\sim 2\text{-}5 \text{ nm}$) in the absorption for all the compounds and in the fluorescence for Cyt and the N1 derivatives.

Comparison of the spectra between Cyt and the N1-derivatives shows that, regardless of the solvent used, the N1-substitution causes slight wavelength red-shifts (by $\sim 5 \text{ nm}$) both in absorption and fluorescence and increases slightly the absorption coefficient and

the quantum yield of fluorescence. On the other hand, in both water and methanol, the methyl substitution at C5 position leads to substantial red-shifts (by ~15-17 nm) in both absorption and fluorescence and elevates significantly (by ~6-7 folds) the fluorescence quantum yield compared to those of Cyt and the counterpart N1 derivatives. This observation agrees well with those reported before for m5Cyd and m5dCyd in water.^[2b,4c]

Table 1 Spectral and dynamic parameters obtained for Cyt and its N1 and C5 derivatives in water and methanol

		^a $\lambda_{\text{Abs}}/\text{nm}$	^b $\epsilon/\text{Lmol}^{-1}\text{cm}^{-1}$	^c λ_f/nm	^d τ_1/ps	^d τ_2/ps	^e τ_3/ps	$a_{\pi\pi^*}\%$ (^f $a_{\text{FC}}\%$, ^g $a_{\text{min}}\%$)	^h $a_{\text{n}\pi^*}\%$	ⁱ $\Phi_f(\times 10^{-4})$
Cyt	H ₂ O	267	6333	^k 322	0.2 ± 0.03	1.5 ± 0.1	7.7 ± 0.6	75 (64, 11) ± 2	25 ± 4	^j 0.82
	CH ₃ OH	268	6221	^l 327	0.2 ± 0.03	1.1 ± 0.1	52 ± 3			
Cyd	H ₂ O	271	9199	325	0.2 ± 0.03	1.8 ± 0.1	35 ± 2	50 (38, 12) ± 4	49 ± 4	1.02 ± 0.06
	CH ₃ OH	273	8816	326	0.3 ± 0.03	1.3 ± 0.1	144 ± 4			1.08 ± 0.07
dCyd	H ₂ O	271	9807	324	0.2 ± 0.03	1.1 ± 0.1	30 ± 2	66 (54, 12) ± 3	33 ± 5	0.89 ± 0.06
	CH ₃ OH	273	8964	326	0.2 ± 0.03	0.8 ± 0.1	186 ± 6			0.83 ± 0.08
CMP	H ₂ O	271	8597	327	0.3 ± 0.03	1.8 ± 0.1	34 ± 2	60 (42, 18) ± 3	39 ± 5	1.52 ± 0.08
dCMP	H ₂ O	271	8879	326	0.2 ± 0.03	1.3 ± 0.1	30 ± 2			1.11 ± 0.05
m5Cyd	H ₂ O	278	8871	341	0.7 ± 0.05	7.6 ± 0.3		99 ± 2		7.53 ± 0.32
	CH ₃ OH	280	7804	341	0.8 ± 0.05	5.1 ± 0.3				7.46 ± 0.30
m5dCyd	H ₂ O	278	9153	340	0.6 ± 0.05	5.4 ± 0.3		99 ± 2		5.97 ± 0.25
	CH ₃ OH	280	7806	340	0.6 ± 0.05	4.1 ± 0.3				5.93 ± 0.28

^aWavelength of ^bthe maximum extinction coefficient in steady state absorption. ^cWavelength of the maximum intensity of steady state fluorescence. Decay time constants derived from ^dfs-TRF and ^efs-TA measurements. Percentage contributions from decay channel ^f $\pi\pi^*_{\text{FC}} \rightarrow \text{S}_0$, ^g $\pi\pi^*_{\text{FC}} \rightarrow \pi\pi^*_{\text{min}} \rightarrow \text{S}_0$, and ^h $\pi\pi^*_{\text{FC}} \rightarrow \text{n}\pi^* \rightarrow \text{S}_0$. ⁱFluorescence quantum yield from ^j[16(b)-(c)]. ^kFrom [16(a)] and ^lfrom [16(d)].

Femtosecond broadband time-resolved fluorescence spectroscopy

Figure 2 depicts the temporal evolutions of fs-TRF spectra, the kinetic decay profiles of TRF intensities, and the zero time fluorescence anisotropy spectra ($r(0)$) recorded with 267 nm excitation of Cyt, Cyd, CMP, and m5Cyd in water. The corresponding data for dCyd, dCMP, and m5dCyd in water and for Cyt, Cyd, dCyd, m5Cyd, and m5dCyd in methanol are given in Figure S2 and S3 in the SI. Figure 3 compares the TRF decay profiles from Cyt, Cyd, and m5Cyd in water vs in methanol. Fs-TRFA spectra recorded for

the various compounds in water and in methanol at different time intervals after the excitation are given in Figure S4 in the SI.

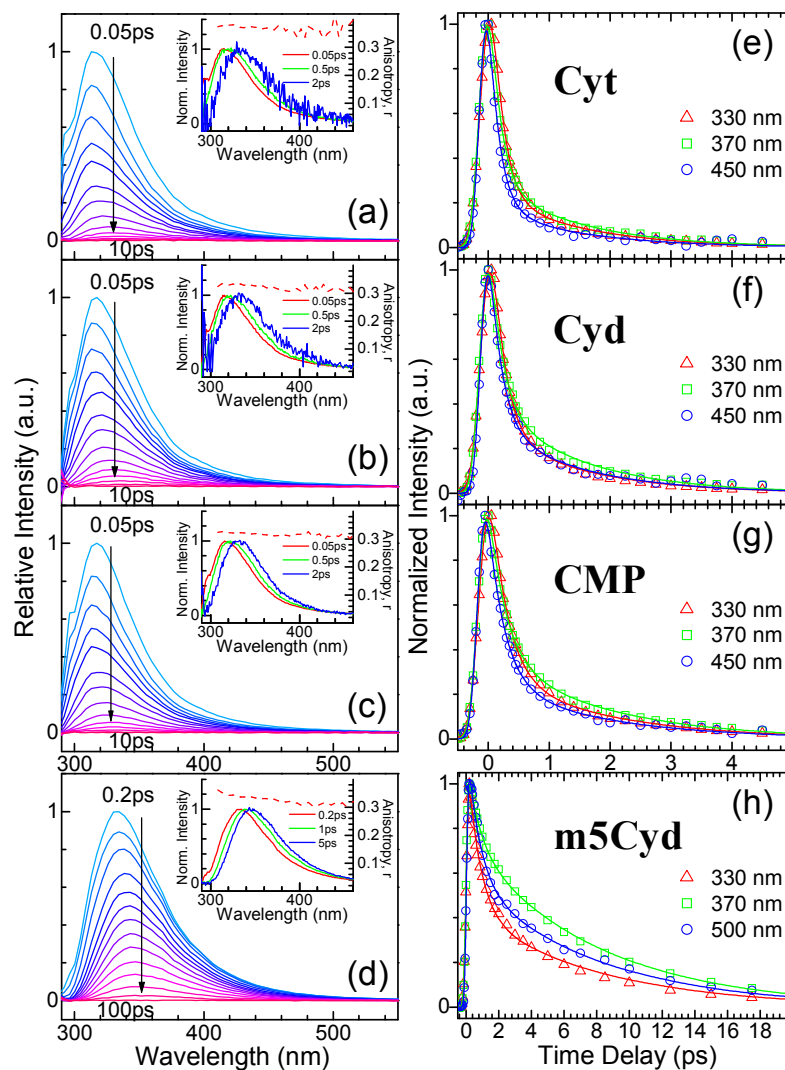


Figure 2. (a-d) fs-TRF spectra and (e-h) experimental (Δ , O , \square) and fitted (solid lines) TRF decay profiles obtained with 267 nm excitation at denoted emission wavelength for (a, e) Cyt, (b, f) Cyd, (c, g) CMP and (d, h) m5Cyd in water. The insets show zero time TRF anisotropy spectra and intensity normalized TRF spectra at the denoted time intervals after the photo-excitation. The arrows indicate directions of spectral evolutions.

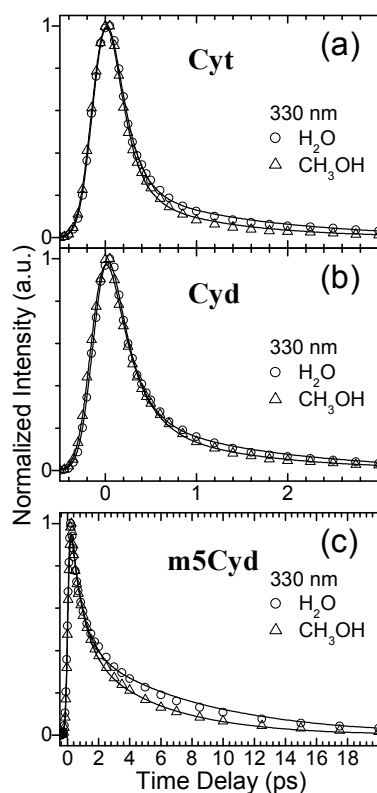


Figure 3. Experimental (O, Δ) and fitted (solid lines) TRF decay profiles obtained with 267 nm excitation at denoted emission wavelength for (a) Cyt, (b) Cyd and (c) m5Cyd in water (O) and in methanol (Δ).

From Figure 2 and Figures S2-S3, it can be seen that, for all the compounds, the fs-TRF spectra in water and in methanol resemble the spectra of the counterpart steady state fluorescence (Figures 1 and S1). Global analysis^[14,15] of the TRF intensity decays demonstrated bi-exponential dynamics described by two time constants (τ_1 and τ_2 , Table 1) for all the systems examined. The detailed values of the time constants and the related fractional contributions ($a_1\%$ for τ_1 , $a_2\%$ for τ_2) at several selected emission wavelengths as well as the values of $r(0)$ are given in Table S1 in the SI.

The fs-TRF (and the steady state fluorescence) from all the compounds in water and methanol (Figure 2 and Figures 2S-3S) can be attributed with certain to originate from the

photo-populated $\pi\pi^*$ state. This is indicated by the data of TRFA (inset in Figures 2 and S2-3, Figure S4) which shows that the anisotropies of transient fluorescence in all systems are nearly independent of the emission wavelength and with the value of time zero anisotropy (~ 0.32 – 0.37 , Table S1) close to the theoretical value of 0.4 when fluorescence is from the same electronic state for absorption in the photo-excitation. The values of the time zero anisotropy we obtained with Cyt (~ 0.37) and dCMP (~ 0.34) in water are nearly identical to those reported in the literature.^[2a-b] It is therefore unequivocal that the TRF, albeit its bi-exponential dynamics, is due from one single state, the light-absorbing $\pi\pi^*$, in all the systems examined.

As showed in Table 1 and Figures 2 and S2-S3, for Cyt and N1-derivatives, the time constants (τ_1/τ_2) of the bi-exponential decays are very similar, being ~ 0.2 - $0.3/1.1$ - 1.8 ps in water and ~ 0.2 - $0.3/0.8$ - 1.1 ps in methanol. The time constants from C5-derivatives are however relatively much slower, being ~ 0.6 - $0.7/5.4$ - 7.6 ps in water and ~ 0.6 - $0.7/4.1$ - 5.1 ps in methanol. For the decay times in water, the values we derived coincide with the those reported in the previous fs-FU studies.^[4a-c]

A clear trend demonstrated by the fs-TRF data is that, for all the compounds investigated, the decays of fluorescence are consistently slightly faster in methanol than in water (Figure 3 and Table 1). With the time constant of the first component (τ_1) being nearly independent of the solvent, this occurs mainly due to the time constant of the second component (τ_2) is slightly more rapid in the former than later solvent.

Examination of the fluorescence decays at the different emission wavelengths shows that, for Cyt and the N1 derivatives, the decays in both water and methanol varied only marginally with the emission wavelength, which is due to the involvement of small degrees (by ~ 10 nm) of dynamic Stokes shift (DSS) of the TRF profiles (insets in Figures 2, S2-3) as decays of the TRF intensities. For all these systems, the decays of fluorescence

proceeded primarily in the sub-ps timescale with $\sim 80\text{--}90\%$ ($a_1\%$) of the overall fluorescence disappeared at the time constant of τ_1 and the remaining $\sim 10\text{--}20\%$ ($a_2\%$) the time constant of τ_2 . Unlike this, the TRF decays of the C5-derivatives (in water or methanol) exhibit clear variations with the emission wavelength (Figure 2h), being slower at longer wavelength. This according to the kinetic fitting is due to increase with the wavelength of the relative contribution of the second time component τ_2 . Such as for m5Cyd in water, the contribution of τ_2 varies from $\sim 31\%$ at 330 nm to $\sim 67\%$ at 370 nm (Table S1). This is in analogous to the complex fluorescence decays reported earlier for the same system.^[4c] To elucidate the deactivation pathway underlying the bi-exponential TRF decays and the cause for the different TRF behaviour between C5-derivatives vs Cyt and N1 derivatives, fs-TA measurements were performed and the results are illustrated below.

Femtosecond broadband transient absorption spectroscopy

Figure 4 displays temporal evolutions of fs-TA spectra recorded in water for Cyt, Cyd, CMP, and m5Cyd at various time intervals after the 267 nm excitation. The corresponding full scale spectra and the spectra for dCyd, dCMP, and m5dCyd in water and for Cyt, Cyd, dCyd, and m5Cyd in methanol are presented respectively in Figure S5 and S6 in the SI. It is clear from these data that, for all these systems, the TA spectra feature the positive-going bands across the visible wavelengths due to the excited state absorption (ESA) and negative-going bands at $\sim 340\text{--}360$ nm due to the stimulated emission (SE) from the $\pi\pi^*$ state and at $< \sim 300$ nm wavelengths due to the S_0 bleach induced from depletion of the S_0 population by the photo-excitation. Kinetic profiles of the TA intensity decays at representative wavelengths for the ESA (e.g. ~ 416 and 570 nm) and the S_0 bleach (e.g. ~ 258 nm) are compared in Figure 5 for Cyt, Cyd, dCyd, and

m5Cyd in water and in methanol and in Figure S7 for the other systems in water. For all the systems examined, the decay time constants derived from global analysis of the TA time profiles are included in Table 1 with the detailed dynamic parameters presented in Table S2 in the SI.

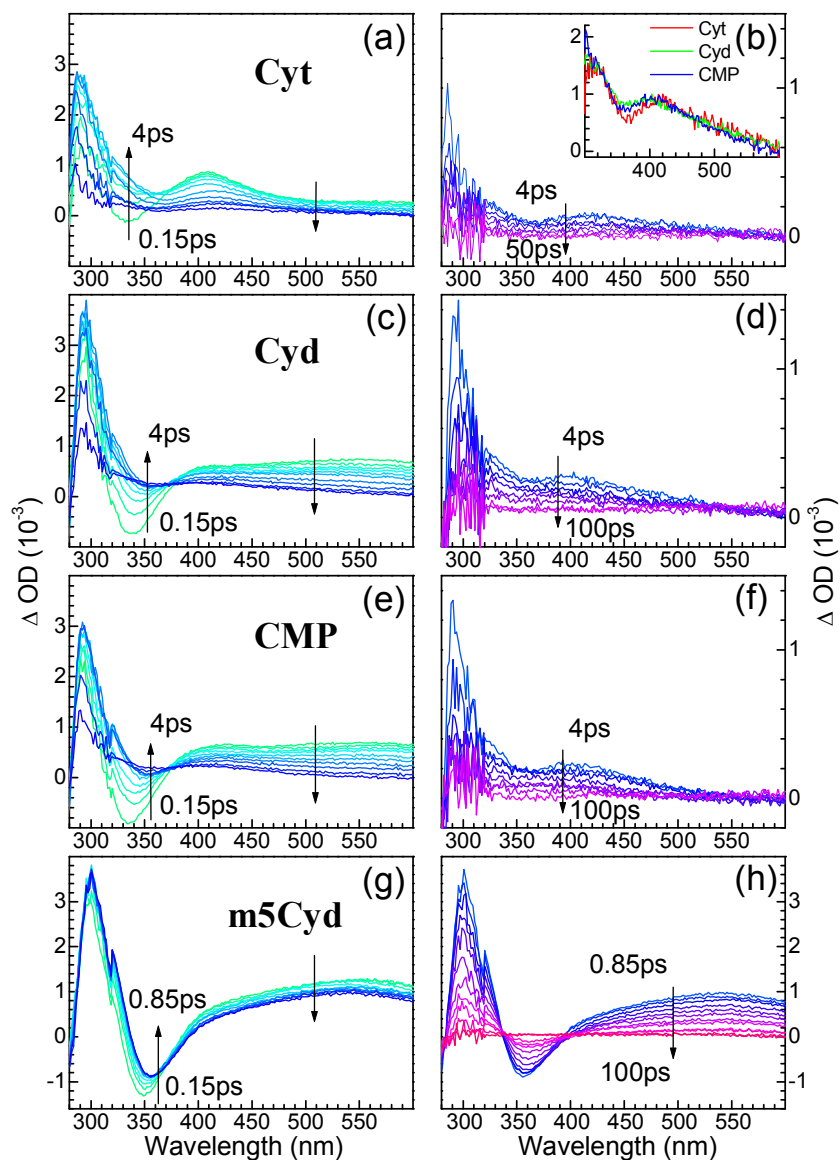


Figure 4. Temporal evolutions of fs-TA spectra recorded at early (left) and late (right) time intervals after 267 nm excitation of (a, b) Cyt, (c, d) Cyd, (e, f) CMP and (g, h) m5Cyd in water. The arrows indicate directions of spectral evolutions. The inset in (b) compares the spectra at ~4 ps after the excitation of Cyt, Cyd and CMP in water.

Femtosecond transient absorption of Cyt and N1 derivatives

Cyt and all its N1-substituted derivatives exhibit fs-TA (Figures 4(a-f) and S5-7) that are very similar in the spectral profile but different in the decay dynamics depending on the solvent used and the presence or not of the ribose or deoxyribose at the N1 position.

Regardless of the solvent used, all these compounds display initial ESA (at 0.15 ps) having a strong band at ~ 300 nm and a weaker and diffuse band at the entire visible region. The spectra, as showed in Figure 4 and S5-6, can be considered to evolve in two phases at time before and after ~ 4 ps after the photo-excitation. In the first phase ($< \sim 4$ ps), the initial ESA depletes rapidly along with diminishing of the SE from $\pi\pi^*$ state. The decay, according to the global analysis (at ~ 570 nm, Figures 5 and S7), is described by the same set of two time constants (τ_1 and τ_2 , Table S2) as that from the decays of TRF in the corresponding system (Table 1 and S1). On the basis of this observation, the early phase decay was attributed to the $\pi\pi^*$ state being detected in both fs-TRF and fs-TA and the initial ESA the absorption characteristic of the $\pi\pi^*$ in Cyt and all the N1 derivatives in both water and methanol.

After the decay of $\pi\pi^*$ state, the TA in the second phase ($> \sim 4$ ps) features ESA at ~ 300 nm and with a new band at $\lambda_{\max} \sim 410$ nm in wavelengths from ~ 300 to 500 nm (the late time spectra in Figures 4, S5-S6). The $\sim 300/410$ nm ESA exhibits decay in different timescales (TA profiles at ~ 416 nm, Figures 5 and S7) with its lifetime (τ_3) determined to be ~ 7.7 ps for Cyt and ~ 30 - 35 ps for the N1 derivatives in water but much slower in methanol being ~ 52 ps for Cyt and $\sim 144/186$ ps for Cyt/dCyt (Table 1 and S2). Unlike that of the $\pi\pi^*$, the decay of $\sim 300/410$ nm ESA has no counterpart in the corresponding fs-TRF (Figures 2 and S2-3), implying its origination from an optically dark species undetectable in the fs-TRF. On the basis of this and that the $\sim 30/34/30$ ps lifetimes we

observed with dCyd/CMP/dCMP in water coincide with the lifetimes of $n\pi^*$ reported for these compounds in the same solvent,^[2c,3] the species was attributed to the $n\pi^*$ and the $\sim 300/410$ nm ESA the absorption signature of the $n\pi^*$ state in the respective compounds.

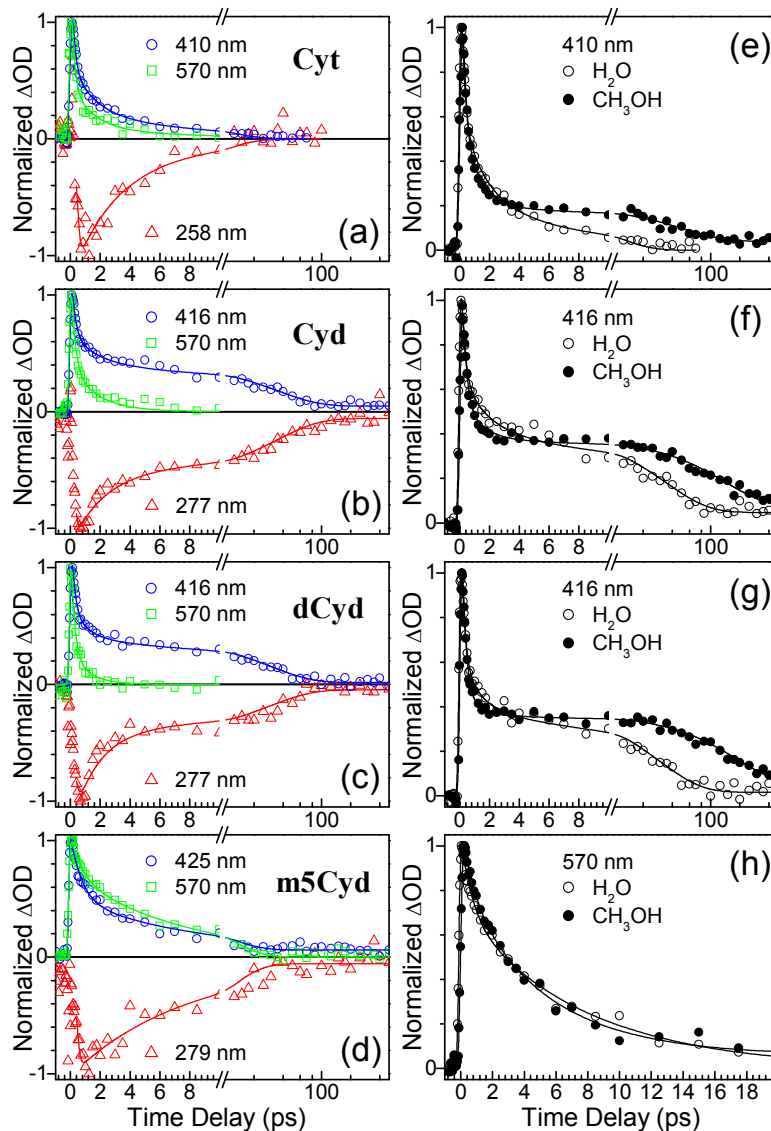


Figure 5. Fs-TA time profiles obtained for (a, e) Cyt, (b, f) Cyd, (c, g) dCyd, and (d, h) m5Cyd in (a-d) water and (e-h) comparison with the corresponding time profiles in methanol.

The observation of $n\pi^*$ signature absorption in the fs-TA of Cyt (insets in Figure 4(b) and Figure S8) provides direct evidence for participation of the $n\pi^*$ in Cyt nonradiative

decay both in water and in methanol. For Cyt and the N1 derivatives, the data we observed in methanol afford the first direct identification of the $n\pi^*$ during the deactivation of these systems in solvent other than water. The large variations in the $n\pi^*$ lifetime from Cyt to N1 derivatives and upon changing solvent from water to methanol testifies remarkable roles of the N1 substitution and the solvent in altering pronouncedly the dynamics of $n\pi^*$ state.

Analysis of the TA time profiles (in water) in the S_0 bleach region (Figures 5 and S7) revealed biphasic recovery of the S_0 caused by decays of the $\pi\pi^*$ and $n\pi^*$ state. For Cyt and all the N1 derivatives, the recovery in the first phase demonstrated time constant of ~ 1.7 - 2.9 ps (Table S2) which was clearly due to relaxation of the vibrationally excited S_0 produced due to rapid decay of the $\pi\pi^*$ to S_0 ($\pi\pi^* \rightarrow S_0$). The ~ 1.7 - 2.9 ps time constants are typical of such process, similar to those reported in the ultrafast studies for the bases in water.^[1a,2c,5a,5b] The relaxation taking place in the S_0 is known to proceed at rates slightly slower than the decay of $\pi\pi^*$ for it is rate-determined by dissipation of excess vibrational energy from the "hot" S_0 to surrounding solvent molecules.^[1a,2,3,5] The percentage recovery due to this process from the decay of $\pi\pi^*$ ($a_{\pi\pi^*}$ %, Table 1) was estimated to be $\sim 75\%$ in Cyt and $\sim 50/66/60\%$ in Cyd/dCyd/CMP in water. On the other hand, being synchronous with the decay of $n\pi^*$ state, the second phase recovery of S_0 is obviously due to the decay of $n\pi^*$ state ($n\pi^* \rightarrow S_0$), which was found to contribute a fraction ($a_{n\pi^*}$ %, Table 1) of $\sim 25\%$ for Cyt and $\sim 49/33/39\%$ for Cyd/dCyd/CMP in water. The substantial contributions from the $n\pi^*$ implies that the $n\pi^*$ competes strongly with the $\pi\pi^*$ for coupling with the S_0 in the deactivation of both Cyt and the N1 derivatives.

A close inspection of the TA spectra (Figures 5 and S7, Table S2) showed that, after the biphasic recovery which altogether amounts $\sim 99\%$ of the overall bleach signal, there was persistence of the remaining $\sim 1\%$ bleach signal over timescale beyond that of current measurement ($> \sim 6$ ns). This implies presence of very long-lived species after the decays

of $\pi\pi^*$ and $n\pi^*$ state. With no involvement of photochemical reaction as suggested by the nearly identical steady state absorption before and after the TA measurement, the species was most likely due to the electronically excited triplet state which may form through spin orbital coupling with the $\pi\pi^*$ or $n\pi^*$ state as proposed by theoretical studies.^[2c,5a,17] This assignment is corroborated by (i) the long-lived nature of the residual signal which according to kinetic analysis is related to a lifetime of $>\sim 20$ ns (Table S2) under the aerated condition in the TA measurement; (ii) its minute contribution ($<\sim 1\%$) which is close to the yields of triplet reported for Cyt and some of its nucleosides and nucleotides;^[18a] and more important (iii) the offset signal was found to correlate dynamically with a weak and broad ESA in the visible wavelengths (Figure S9) which resemble the literature spectra reported for the triplet state of Cyt, Cyd, and dCMP in water.^[18b-d]

The above results taken together show clearly that, for Cyt and all the N1 derivatives, the nonradiative decays occur predominantly in the singlet manifold mediated by both the $\pi\pi^*$ and $n\pi^*$ state with the respective contribution of $a_{\pi\pi^*}\%$ and $a_{n\pi^*}\%$ (Table 1) and in the timescale of sub-picosecond to picosecond for the decay of $\pi\pi^*$ state (τ_1, τ_2) and several to hundreds picoseconds for the $n\pi^*$ state (τ_3) depending on the solvent. The deactivation, referred to proceed through a two-state pathway, is diagrammed in Scheme 2(a).

Femtosecond transient absorption of C5 derivatives

It can be seen from Figure 4 and S5-S6 that, unlike Cyt and the N1 derivatives, the C5 derivatives (m5Cyd and m5dCyd) in both water and methanol display fs-TA without the $\sim 300/410$ nm absorption due to $n\pi^*$ state. Instead, the fs-TA of the C5-derivatives exhibit ESA and bleach recovery primarily due to the light-absorbing $\pi\pi^*$ state.

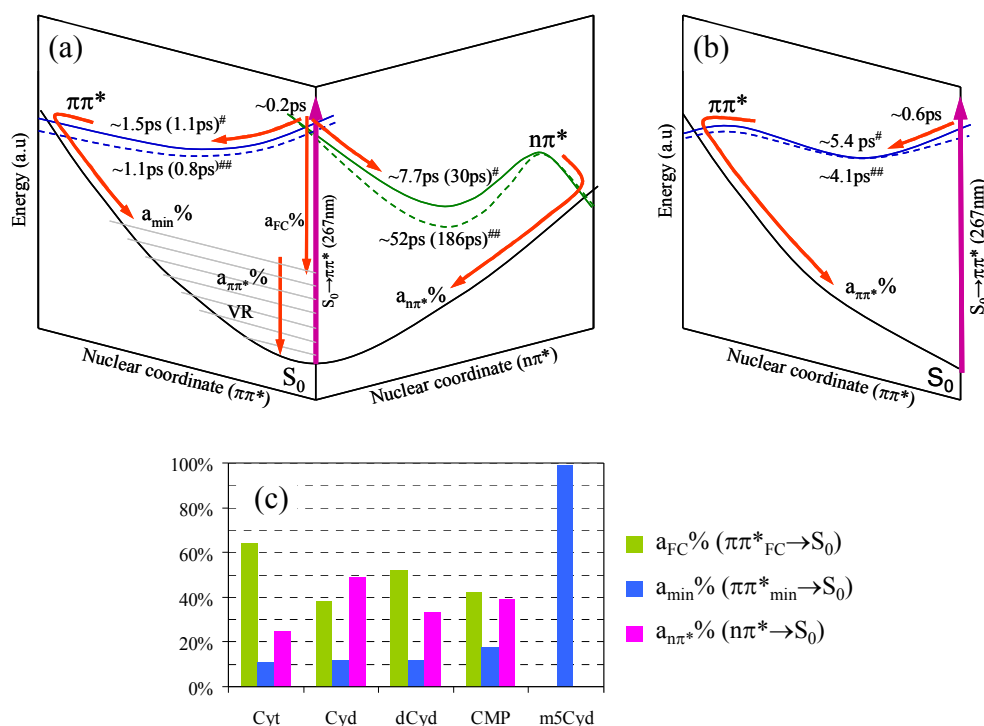
The ESA features the broad absorption characteristic of the $\pi\pi^*$ which decays along with depletion of the SE from $\pi\pi^*$ state. The decay of ESA demonstrated bi-exponential dynamics with the time constants (τ_1 and τ_2 , Table S2) identical to those from the corresponding fs-TRF (Figures 2(h), S2-3, Table S1). The S_0 bleach, on the other hand, exhibits recovery described by mono-exponential dynamics with time constant equivalent to the τ_2 of the excited state decay. After the recovery at τ_2 of most the bleach signal, there is persistence of a small percentage ($<\sim 1\%$) of long-lived residual (Figure 4 and Table S2) which can be attributed to the triplet state of the C5 derivatives by analogy to the case of Cyt and N1 derivatives.

With the minute involvement of the long-lived triplet state, it is straightforward that the decay at τ_2 of the $\pi\pi^*$ state is the major process responsible for transferring the excited state population into the S_0 . Within this context, the τ_1 related process in both ESA and TRF can be ascribed to relaxation of the $\pi\pi^*$, which as suggested by the nearly solvent-independent DSS (inset in Figures 2(d) and S2-3) can be attributed to the structural relaxation of the initial $\pi\pi^*$ ($\pi\pi^*_{FC}$) as it evolving from the FC region to the region where the state crossover occurred. Considering the rather long lifetime of $\pi\pi^*$ state (~ 4.1 - 7.6 ps, Table 1), the conversion to S_0 is most likely taking place after the $\pi\pi^*$ relaxed into the local minimum of its PES ($\pi\pi^*_{min}$).

Therefore, for the C5 derivatives, the nonradiative decays proceeded as a result of the $\pi\pi^*_{FC} \rightarrow \pi\pi^*_{min}$ relaxation at the time constant of τ_1 followed by the $\pi\pi^*_{min} \rightarrow S_0$ crossover at τ_2 . The deactivation is therefore referred to occur through a *one-state* pathway ($\pi\pi^*_{FC} \rightarrow \pi\pi^*_{min} \rightarrow S_0$) mediated solely by the $\pi\pi^*$ state and is illustrated in Scheme 2(b).

DISCUSSION

The fs-TRF, fs-TRFA, and fs-TA results we obtained show that, in both water and methanol, there are two types of nonradiative cascades, the *two-state* pathway from the $\pi\pi^*$ and $n\pi^*$ for Cyt and its N1 derivatives and the *one-state* channel from the $\pi\pi^*$ for the C5-derivatives. The deactivation of $\pi\pi^*$ and $n\pi^*$ is affected distinctively by the solvent. Varying solvent from water to methanol accelerates slightly the decay of $\pi\pi^*$ but retards strongly the deactivation of $n\pi^*$ state (Scheme 2).



Scheme 2. Proposed nonradiative decay channels for (a) Cyt and N1 derivatives and (b) C5 derivatives in water (solid line) and in methanol (dash line). The time constants in (a) are from Cyt(dCyd) and in (b) from m5dCyd in [#]water and ^{##}methanol. VR = vibrational relaxation. (c) Percentage contribution of the channels from $\pi\pi^*$ ($a_{\pi\pi^*}\% = a_{FC}\% + a_{\min}\%$) and $n\pi^*$ ($a_{n\pi^*}\%$) state to the overall deactivation of the denoted compounds in water.

However, for the case of Cyt and N1 derivatives, to ascertain the details of the decay of $\pi\pi^*$ and the origin of $n\pi^*$, it is instructive to examine any correlation between the fractions of S_0 recovery caused by the $\pi\pi^*$ and $n\pi^*$ ($a_{\pi\pi^*}\%$ and $a_{n\pi^*}\%$) versus those

involved in the bi-exponential decay of photo-prepared $\pi\pi^*$ state ($a_1\%$ and $a_2\%$) as revealed in the fs-TRF (Figures 2, S2, S3, and Table 1). It is noted in this regard that the $a_{\pi\pi^*}\%$ and $a_{n\pi^*}\%$ are both smaller than the fraction of $\pi\pi^*$ population ($a_1\% \sim 80-90\%$) deactivated at the time constant of $\tau_1 \sim 0.2-0.3$ ps but are greater than those ($a_2\% \sim 10-20\%$) at the time constant of $\tau_2 \sim 0.8-1.8$ ps. This is indicative of two important features. *First*, the $\pi\pi^* \rightarrow S_0$ conversion is most likely occurring in two timescales from two different regions of the $\pi\pi^*$ PES: one in the sub-picosecond timescale with the time constant of τ_1 from area close to the Franck-Condon region ($\pi\pi^*_{FC} \rightarrow S_0$), and the other is a sequential process which, as suggested by the DSS in fs-TRF, may proceed after relaxation of the initial $\pi\pi^*$ to a local minimum ($\pi\pi^*_{FC} \rightarrow \pi\pi^*_{min}$)^[6c] where the conversion ($\pi\pi^*_{min} \rightarrow S_0$) occurred at the time constant of τ_2 . With the fraction in the $\pi\pi^*_{min} \rightarrow S_0$ channel (denoted as $a_{min}\%$) having a value corresponding to the $a_2\%$ (i.e., $a_{min}\% = a_2\%$), the fractional population along the $\pi\pi^*_{FC} \rightarrow S_0$ channel (denoted as $a_{FC}\%$) can be estimated ($a_{FC}\% = a_{\pi\pi^*}\% - a_{min}\%$) to be $\sim 64\%$ for Cyt and $\sim 38/54/42\%$ for Cyd/dCyd/CMP in water (Table 1). The two $\pi\pi^*$ channels, masked by the slower rate-determining energy relaxation of the vibrationally excited S_0 ,^[1-2,5] manifested themselves as a single step to account for the first phase S_0 recovery as observed in the fs-TA. The *second* important feature is that, the longer-lived $n\pi^*$ state, dark and not directly accessible by the photo-excitation, must become involved in the sub-picosecond timescale through coupling with the initial $\pi\pi^*$ ($\pi\pi^*_{FC} \rightarrow n\pi^*$). This coupling competes with the channel of $\pi\pi^*_{FC} \rightarrow S_0$ and jointly ($a_{FC}\% + a_{n\pi^*}\% \approx a_1\%$) they were responsible for the massive decrease of the $\pi\pi^*$ population observed at the time constant of $\tau_1 \sim 0.2-0.3$ ps. Therefore, for all these compounds, the nonradiative decays, though mediated by the *two-state pathway*, occurred actually through *three-channels* leading from the $\pi\pi^*_{FC}$, $\pi\pi^*_{min}$, and $n\pi^*$ state with the fractional contribution of $a_{FC}\%$, $a_{min}\%$, and $a_{n\pi^*}\%$ and the corresponding time constant of τ_1 , τ_2 , and τ_3 , respectively (Scheme 2(a)). On the basis of this, the deactivation of Cyt and N1-derivatives is regarded

as following a *two-state-three-channel* model. Along this line, the deactivation of C5-derivatives is referred to proceed through a *one-state-one-channel* model ($\pi\pi^*_{FC} \rightarrow \pi\pi^*_{min} \rightarrow S_0$) as diagrammed in the Scheme 2(b) and (c).

Whilst the operation of multiple decay channels from $\pi\pi^*$ and $n\pi^*$ has been accepted widely for Cyt in the gas phase,^[7-11] the situation in the solution phase is much less understood. Our study, thanks to the ability to probe nearly all the possibly involved species (bright or dark) in solvents of varied polarity and H-bonding capacity, allows unveiling several unprecedented traits for the evolutions of excited states and roles of solvent and substitution in affecting distinctively the dynamics and pathways of Cyt nonradiative decays.

Nonradiative dynamics of Cyt

For Cyt, the *two-state-three-channel* pathway provides a unifying picture for explaining the bi-exponential dynamics of $\pi\pi^*$ and the interplay of $\pi\pi^*$ with $n\pi^*$ to jointly account for the nonradiative decays in solution. The direct observation of $n\pi^*$ state in the fs-TA (Figures 4-5) provides unambiguous evidence for clarifying the divergence in literature^[2c,3] and verifies the involvement of the $n\pi^*$ in the solution phase nonradiative deactivation. In addition, despite agreeing with earlier studies in regarding the presence of $\pi\pi^*$ to S_0 conversion on the ~ 1 ps timescale,^[2,3] our data show that such a process (corresponding to the $\pi\pi^*_{min} \rightarrow S_0$ channel) makes only limited contribution ($a_{min}\% \sim 11\%$, Table 1) to the overall decay, while most of the conversion from $\pi\pi^*$ to S_0 occurred actually in the sub-ps timescale through the direct channel $\pi\pi^*_{FC} \rightarrow S_0$ ($a_{FC}\% \sim 64\%$, $\tau_1 \sim 0.2$ ps) competing with the formation of $n\pi^*$ state ($\pi\pi^*_{FC} \rightarrow n\pi^*$) which deactivated ($n\pi^* \rightarrow S_0$) on the much slower timescale from several to tens ps depending on the solvent.

One determining step in the *two-state-three-channel* model is the splitting in hundreds fs of the photo-prepared $\pi\pi^*$ population into the S_0 , the $n\pi^*$, and the structurally relaxed $\pi\pi^*$ state (Scheme 2(a)). This in the other words means coexistence of multiple and nearly barrierless decay paths from the initial $\pi\pi^*$ to the $n\pi^*$ and the S_0 , which is in principle consistent with the theoretical studies on Cyt in the gas phase showing the presence of several CIs connecting in nearly barrierless manner between the $\pi\pi^*$, $n\pi^*$, and S_0 .^[7,9-11] In this regard, the two $\pi\pi^*$ channels in our model can be associated to the two mostly reported CIs with the out-of-plane twisting of C5-C6 bond and the semi-planar stretching of C5-C6 bond for the crossover from $\pi\pi^*$ to S_0 .^[6,8,9]

On the other hand, between the two possible $n\pi^*$ states having the lone pair electrons from the N3 ($n_N\pi^*$) and O7 ($n_O\pi^*$),^[6c,d,h,7,9,16a] the state we observed is mostly likely corresponding to the $n_O\pi^*$. According to the theoretical studies,^[9] the $n_O\pi^*$ at its energy minimum geometry is the lowest energy excited state in the singlet manifold and plays an important role in the deactivation of Cyt in the gas phase. The $n_N\pi^*$ state, lying already at higher energy (than both $\pi\pi^*$ and $n_O\pi^*$) in the gas phase, is less probable to be involved in the decays in solution for the state is expected to be further destabilized by interaction with solvent in the solution phase.^[1,4d-f,8a-b,14a,19] Pertinent to this, it is noted that, although originally ascribed to the $n_N\pi^*$,^[3a] the $n\pi^*$ state observed in the ps-TRIR for dCyt and dCMP in water was later re-assigned to the state of $n_O\pi^*$.^[3b]

Occurring in the gas phase^[7,9,12c] and also in the solution as demonstrated here, the multiple path nonradiative decay through $\pi\pi^*$ and $n\pi^*$ is clearly *an intrinsic property of Cyt regardless of the environmental condition*. Given that the $\pi\pi^*$ and $n\pi^*$ usually response very differently to solvent and covalent substitution, the data we obtained for Cyt in water provides a benchmark for assessing effects of solvent and the N1 and C5 substitution on the dynamics and pathways of the Cyt deactivation.

Effects of N1-substitution

An obvious result from comparing the data between Cyt and the N1 derivatives is that the substitution at N1 alone by ribose or deoxy-ribose with or without the phosphate moiety *makes no qualitative difference* to the overall pattern of Cyt nonradiative decay. All the examined N1 derivatives share with Cyt the *two-state-three-channel* pathway (Scheme 2). This is in contrast with ps-TRIR studies^[3] which reported deactivation through both the $\pi\pi^*$ and $n\pi^*$ for the N1 derivatives (dCyt and dCMP) but through only the $\pi\pi^*$ state for the case of Cyt. According to our data, the N1 substitution causes important *but only quantitative* changes to the deactivation of Cyt.

The most significant change arising due to the N1 substitution is that it affected the ultrafast (in ~ 0.2 ps) branching of the initial $\pi\pi^*$ population, favouring the channel of $n\pi^*$ state. This is manifested by the increase in both the efficiency ($a_{n\pi^*}$ %) and the lifetime (τ_3) of the $n\pi^*$ channel from such as $\sim 25\%$ and 7.7 ps in Cyt to $\sim 33-49\%$ and $\sim 30-35$ ps in the N1 derivatives. This observation is consistent with the general trend reported for the pyrimidine bases in water.^[2c] However, as a novel feature, our data shows that the increase of $n\pi^*$ efficiency occurs since the N1 substitution suppresses effectively the ultrafast $\pi\pi^*_{FC} \rightarrow S_0$ channel (a_{FC} % $\sim 64\%$ in Cyt to 38-52% in N1 derivatives, Table 1) allowing enhanced formation of the $n\pi^*$ in as early as ~ 200 fs after the excitation. The long lifetime of $n\pi^*$ implies the $n\pi^*$ possessing a well defined energy minimum separated by a sizeable energy barrier from the S_0 . The lengthening of $n\pi^*$ lifetime reflects that the N1 substitution raised the barrier height and slowed down the barrier crossing to the S_0 . With the N1 substitution to strengthen its the ultrafast coupling with the initial $\pi\pi^*$ and at the same time to retard it from deactivated into the S_0 , the $n\pi^*$ of N1-derivatives is clearly a more effective trap to the excitation than that of Cyt, implying an important role of the $n\pi^*$ in the photostability and photochemistry of DNA and RNA.

In contrast to the $n\pi^*$ state, the $\pi\pi^*$ state exhibited decays with the rates fairly similar between Cyt and the N1 derivatives. This suggests very limited influence of the N1 substitution on the $\pi\pi^*/S_0$ crossover.

The distinctive influence of N1 substitution on the $n\pi^*$ vs $\pi\pi^*$ state suggests that the decays into S_0 from the two states must proceed through different nuclear coordinates especially in terms of the atoms involved in the ribose or deoxyribose moiety. In spite of the large number of sophisticated theoretical studies on the nonradiative dynamics of Cyt,^[6-9,17] there has been very limited study on its N1 derivatives^[20] and no known comparable work on the nucleosides and nucleotides of Cyt in either the gas phase or solution to the best of our knowledge.

Effects of C5-substitution

According to our results, the presence of an extra methyl at the C5 position removes completely both the ultrafast $\pi\pi^*$ channel ($\pi\pi^*_{FC} \rightarrow S_0$) and the channel due to the $n\pi^*$ state ($n\pi^* \rightarrow S_0$). The substitution, on the other hand, prolongs substantially (by ~4-5 times) the decay of the stepwise $\pi\pi^*$ channel ($\pi\pi^*_{FC} \rightarrow \pi\pi^*_{min} \rightarrow S_0$), making it the sole path for transferring the population from excited state into the S_0 (Scheme 2(b)). Making correlation of the dynamics between fs-TRF and fs-TA shows explicitly that the complex fluorescence decays reported previously for m5dCyd in water,^[4c] which is similarly observed in our measurement for both m5dCyd in methanol and m5Cyd in both water and methanol, is actually occurring due to relaxation of the excited state population within the $\pi\pi^*$ state, bearing no relevance to the state of $n\pi^*$. In this regard, instead of the substitution at N1, it is the C5 substitution that governs the participation or not of the $n\pi^*$ state in the nonradiative decays. The *one-state-one-channel* pathway adopted by m5Cyd and m5dCyd can therefore be considered a special case of the *two-state-three-channel*

pathway by Cyt and N1 derivatives, emphasizing a key role of the C5 substitution in altering the fundamental pattern of the nonradiative decay.

The slower decay of $\pi\pi^*$ in C5 derivatives provides explanation to the higher fluorescence quantum yield of the C5 derivatives than those of Cyt and the N1 derivatives (Table 1) and is supported by theoretical studies showing the involvement of the C5 atom in the $\pi\pi^*/S_0$ conversion. Indeed, as mentioned above, the C5 involved out-of-planar C5-C6 twisting or semi-planar C5-C6 stretching is among the most relevant reaction coordinates for achieving the switch from $\pi\pi^*$ to S_0 . The methyl at C5, presumably through the hyper-conjugation with the pyrimidine ring π system,^[4d,4f,21] may impose restraint to the required change in the C5-C6 bond and slow down the access to related CIs($\pi\pi^*/S_0$) for the state conversion.

As for the elimination of $n\pi^*$ channel in the C5 derivatives, while this may likewise be ascribed to the C5 atom being also involved significantly in the nuclear coordinates for the $\pi\pi^*/n\pi^*$ coupling, an alternative explanation is that the methyl at C5 may cause a preferential stabilization of the $\pi\pi^*$ to $n\pi^*$, which may in turn shift the relative energy or even reverse the energetic ordering of the two states, leaving the $n\pi^*$ at relatively high energy, unavailable for the decay process. Indeed, the steady state absorption and fluorescence of the C5 derivatives are substantially red-shifted from those of Cyt and the N1-derivatives (Figure 1 and Table 1), suggesting energy stabilization of the $\pi\pi^*$ by the methyl at C5 position. Further study in particular at the theoretical perspective would help in assessing the nuclear coordinates for the lack of $n\pi^*$ state in the deactivation of C5 derivatives.

It is remarkable to note that the wavelength red-shift in absorption of C5-derivatives in relative to Cyt and the N1 derivatives has been invoked responsible for the increased mutation rate in the m5dCyd containing DNAs, a phenomenon relevant to the DNA

methylation and the mutation hotspot in skin tumors.^[2b,4c,13] A recent study suggests, however, that the presence of extra methyl at the C5 position may alter the conformation of DNA and as a result affecting the reactivity of $\pi\pi^*$ which may lead to an increased yield of cyclobutane dimers (CPDs),^[22] a major photoproducts for inducing the skin tumors.^[13] Given the absence of the $n\pi^*$ and the $\pi\pi^*$ being the intimate precursor to the CPDs formation, the longer $\pi\pi^*$ lifetime we observed with the C5 derivatives could be another factor contributing to the greater yield of CPDs and the elevated mutation rate in the methylated DNA.

Effects of solvent

The variations in the decay dynamics we observed for Cyt and the derivatives in water vs in methanol exemplify a striking *state specific effect* of the solvent on nonradiative decays. For all the compounds investigated, without affecting the overall deactivation pattern, changing solvent from water to methanol accelerates slightly the rate of $\pi\pi^*$ channel ($\pi\pi^*_{\min} \rightarrow S_0$, τ_2). For Cyt and the N1 derivatives, this change of solvent also retards strongly the decay of $n\pi^*$, extending its lifetime by ~ 4 - 6 folds, from e.g. ~ 7.7 ps (in water) to ~ 52 ps (in methanol) for Cyt and ~ 30 ps (in water) to ~ 186 ps (in methanol) for dCyd.

The effect of solvent we observed with the $\pi\pi^*$ state suggests that the $\pi\pi^*_{\min} \rightarrow S_0$ conversion, albeit being a feasible low or nearly barrierless process as indicated by its rapid rate,^[1a,c,6-9] is less favoured to a subtle but definite degree in the highly polar water (dielectric constant $\epsilon = 78.3$) than in methanol ($\epsilon = 32.7$). This may originate from a different influence of the solvent on the energy of $\pi\pi^*$ in relative to the S_0 . According to the steady state spectra (Figures 1 and S1, Table 1), the absorption (of all the compounds) and fluorescence (of Cyt and the N1 derivatives) of the $\pi\pi^*$ state both exhibit bathchromic

shifts in solvent from water to methanol. This implies that the $\pi\pi^*$ is energetically better stabilized than the S_0 upon decreasing the solvent polarity, which is indicative of the $\pi\pi^*$ possessing a dipole moment smaller than the S_0 ,^[19] supported by the theoretical calculation on solvatochromic shift of Cyt.^[8b] The better stabilization of $\pi\pi^*$ in the less polar methanol may not only occur in the FC region to account for the lower optical transition energy to or from the S_0 , it may also affect the location and topography of the CI ($\pi\pi^*/S_0$), contributing to the slightly faster conversion rate than that in water (Scheme 2). The fact that all the compounds show similar effect of solvent on the sequential $\pi\pi^*$ decay suggests that the related CI ($\pi\pi^*/S_0$) may feature similar electronic and conformation structure irrespective of the N1 and C5 substitution.

It is relevant to note that, for all the compounds in both water and methanol, the fs-TRF (Figures 2 and S2-3) exhibited DSS in time scale associated mainly with the τ_1 (~ 0.2 for Cyt and the N1-derivatives and ~ 0.6 ps for the C5-derivatives). According to the literatures,^[14,15,23] the time-dependent shifts of fluorescence in such time regimes may arise from an ensemble of processes including such as the intramolecular vibrational relaxation, structural relaxation, and dynamic solvation due to reorientation of solvent molecules towards the newly formed excited state (the $\pi\pi^*$ in the current case). However, in view of that the extents of DSS are independent of the solvent (being ~ 10 cm⁻¹ in both water and methanol) and the timescales of DSS are either much slower or much faster than the time of solvation (~ 50 fs for water and ~ 13 ps for methanol),^[23] the dynamic solvation is considered playing a minute role in contributing to the time-dependent fluorescence red-shifts exhibited by Cyt and all the derivative. On the other hand, as mentioned above and supported by theoretical studies,^[6-11] the DSS we observed may arise mainly due to the structural changes of $\pi\pi^*$ state upon evolving from the FC region towards the local energy minimum of its PES. This is consistent with the recent fs fluorescence investigation on the nucleosides and nucleotides of guanine which reported

similar time-dependent fluorescence red-shifts attributed to conformation relaxation and diffusion of excited state population along the PES of the $\pi\pi^*$ state.^[4g,5c]

Unlike the $\pi\pi^*$ state which is affected mainly by the electrostatic interaction with solvent, the state of $n\pi^*$ is energetically sensitive to both the nonspecific electrostatic interaction and more importantly the specific H-bonding with solvent molecules which may typically destabilize the $n\pi^*$ in relative to S_0 .^[4d,4e,4f,19,24] Compared to water, methanol is much less polar and with weaker capacity of H-bonding. The $n\pi^*$ state at its energy minimum is thus expected to be better stabilized and thereby associate with a greater barrier height for the $n\pi^*/S_0$ crossover in methanol than in water, explaining the longer lifetimes of the $n\pi^*$ in the former than latter solvent (Scheme 2).

It is worth noticing that, for Cyt, the change of solvent (from water to methanol) and the presence of N1 substitution appear to have similar effects on the dynamics of $n\pi^*$, both extending the lifetime of $n\pi^*$ and to comparable degrees. Instead of being just a coincidence, this might suggest a certain interplay between the solvent and the N1 substitution in affecting the $n\pi^*/S_0$ coupling. Indeed, the ribose or deoxyribose group, which is sterically bulky, can itself interact extensively with the solvent through both the electrostatic and H-binding interactions.^[25] The extra attachment of this group at the N1 position may thus disturb the microscopic solvation configuration of the pyrimidine moiety, reducing its exposure and weakening its interaction to the solvent. As a result, even in the same solvent, the local solvation experienced by the $n\pi^*$ in the N1 derivatives could be less intense than that in Cyt, and thus the $n\pi^*$ in the former compounds is better stabilized, contributing to its longer lifetime than in Cyt. Note that, although the involvement of low lying CI($n\pi^*/S_0$) has been suggested in many theoretical studies for Cyt in the gas phase,^[7,9,6] the feasibility of the $n\pi^*/S_0$ coupling for Cyt in solution of varied properties and how this is affected by the N1-substitution have remained largely unknown before this work.

CONCLUSION

The excited states of Cyt and the full set of its DNA and RNA nucleosides and nucleotides as well as the C5 methylated nucleosides were studied using fs-TRF, fs-TRFA, and fs-TA in conjunction with steady state absorption and fluorescence in water and methanol. The results clarified the uncertainty on the $n\pi^*$ state and revealed a common *two-state-three-channel* pathway from the $\pi\pi^*$ and $n\pi^*$ for nonradiative decays of Cyt and its N1 derivative in both water and methanol. A *one-state-one-channel* pathway from the $\pi\pi^*$ state was identified for the decays of C5 derivatives. Comparison of the data obtained for Cyt and the derivatives in the different solvents demonstrated remarkable effects of solvent and the N1 and C5 substitution in shaping distinctively the nonadiabatic couplings between the $\pi\pi^*$, the $n\pi^*$, and the S_0 for deactivation in timescale varying from sub-ps to hundreds ps after the excitation. The data we obtained allows improved characterization of the photophysics and provide direct experimental parameters for development of theoretical modelling on influences of solvent and substitution on the topographies of the excited state PESs and dynamics of the nonradiative decays. The results may also help understanding the photostability and photodamage of Cyt and the derivatives. In particular, given the widely documented sub-ps to ps excited state lifetimes of the nucleobases, the $\sim 186/144$ ps lifetime we observed with the $n\pi^*$ state of dCyd/Cyd in methanol is an unusual feature. While such a long lifetime may certainly increase the propensity towards photochemical modification, the $n\pi^*$ state might play a minimal role in the photochemistry but on the other hand may contribute importantly to the photostability of DNA in its canonical form. This is inferred since the canonical DNA is generically much less prone to photodamage than their methylated counterpart where the contained m5dCyd component, according to our result, possesses a longer-lived $\pi\pi^*$ state but with no involvement of the $n\pi^*$ state during the course of excited state decay.

Supporting Information

Details of the materials and the time-resolved measurements and spectral correction for fs-TRF, fs-TRFA, and fs-TA; steady state absorption and fluorescence spectra of Cyt and its derivatives in water; fs-TRF spectra and TRF decay profiles for dCyd, dCMP and m5dCyd in water and for Cyt, Cyd, dCyd, m5Cyd, and m5dCyd in methanol; fs-TRFA spectra for Cyt, Cyd, dCyd, CMP, dCMP, m5Cyd, and m5dCyd in water and methanol; fs-TA spectra and TA time profiles of Cyt, Cyd, dCyd and m5Cyd in water and methanol and of dCyd, dCMP and m5dCyd in water; detailed spectral and dynamic parameters obtained from the fs-TRF, fs-TRFA and fs-TA measurements for Cyt and its N1- and C5-substituted derivatives in water and methanol. This material is available free of charge via the Internet at <http://dx.doi.org>.

Corresponding Author

E-mail: macs@szu.edu.cn; wm.kwok@polyu.edu.hk

ACKNOWLEDGMENT

We thank the National Natural Science Foundation of China (No. 21473114) and the Research Grants Council of Hong Kong (PolyU/5009/11P and PolyU/5009/13P) and Hong Kong Polytechnic University (A-PH84 and A-PK17) for the financial supports.

REFERENCES

- (1) (a) C. E. Crespo-Hernández, B. Cohen, P. M. Hare, B. Kohler, *Chem. Rev.* 2004, **104**, 1977-2019. (b) C. T. Middleton, K. de La Harpe, C. Su, Y. K. Law, C. E. Crespo-Hernández, B. Kohler, *Annu. Rev. Phys. Chem.* 2009, **60**, 217-239. (c) T. Gustavsson, R. Improta, D. Markovitsi, *J. Phys. Chem. Lett.* 2010, **1**, 2025-2030.
- (2) (a) J.-M. L. Pecourt, J. Peon, B. Kohler, *J. Am. Chem. Soc.* 2001, **123**, 10370-10378. (b) R. J. Malone, A. M. Miller, B. Kohler, *Photochem. Photobiol.* 2003, **77**, 158-164. (c) M. P. Hare, C. E. Crespo-Hernández, B. Kohler, *Proc. Natl. Acad. Sci. USA* 2007, **104**, 435-440.
- (3) (a) S. Quinn, G. W. Doorley, G. W. Watson, A. J. Cowan, M. W. George, A. W. Parker, K. L. Ronayne, M. Towrie, J. M. Kelly, *Chem. Commun.* 2007, 2130-2132. (b) P. M. Keane, M. Wojdyla, G. W. Doorley, G. W. Watson, I. P. Clark, G. M. Greetham, A. W. Parker, M. Towrie, J. M. Kelly, S. J. Quinn, *J. Am. Chem. Soc.* 2011, **133**, 4212-4215.
- (4) (a) D. Onidas, D. Markovitsi, S. Marguet, A. Sharonov, T. Gustavsson, *J. Phys. Chem. B* 2002, **106**, 11367-11374. (b) A. Sharonov, T. Gustavsson, V. Carré, E.

- Renault, D. Markovitsi, *Chem. Phys. Lett.* 2003, **380**, 173-180. (c) A. Sharonov, T. Gustavsson, S. Marguet, D. Markovitsi, *Photochem. Photobiol. Sci.* 2003, **2**, 362-364. (d) T. Gustavsson, A. Banyasz, E. Lazzarotto, D. Markovitsi, G. Scalmani, M. J. Frisch, V. Barone, R. Improta, *J. Am. Chem. Soc.* 2006, **128**, 607-619. (e) T. Gustavsson, N. Sarkar, E. Lazzarotto, D. Markovitsi, V. Barone, R. Improta, *J. Phys. Chem. B* 2006, **110**, 12843-12847. (f) F. Santoro, V. Barone, T. Gustavsson, R. Improta, *J. Am. Chem. Soc.* 2006, **128**, 16312-16322. (g) F.-A. Miannary, T. Gustavsson, A. Banyasz, D. Markovitsi, *J. Phys. Chem. A* 2010, **114**, 3256-3263. (h) F. J. Avila Ferrer, F. Santoro, R. Improta, *Comp. Theor. Chem.* 2014, **1040-1041**, 186-194.
- (5) (a) P. M. Hare, C. E. Crespo-Hernández, B. Kohler, *J. Phys. Chem. B* 2006, **110**, 18641-18650. (b) C. T. Middleton, B. Cohen, B. Kohler, *J. Phys. Chem. A* 2007, **111**, 10460-10467. (c) C. C. W. Cheng, C. Ma, C. T. L. Chan, K. Y. F. Ho, W. M. Kwok, *Photochem. Photobiol. Sci.* 2013, **12**, 1351-1365.
- (6) (a) L. Serrano-Andrés, M. Merchán, *J. Photochem. Photobiol. C* 2009, **10**, 21-32. (b) M. Merchán, R. Gonzalez-Luque, T. Climent, L. Serrano-Andres, E. Rodriiguez, M. Reguero, D. Pelaez, *J. Phys. Chem. B* 2006, **110**, 26471-26476. (c) M. Merchán, L. Serrano-Andrés, *J. Am. Chem. Soc.* 2003, **125**, 8108-8109. (d) N. Ismail, L. Blancafort, M. Olivucci, B. Kohler, M. A. Robb, *J. Am. Chem. Soc.* 2002, **124**, 6818-6819. (e) L. Blancafort, M. A. Robb, *J. Phys. Chem. A* 2004, **108**, 10609-10614. (f) A. L. Sobolewski, W. Domcke, *Phys. Chem. Chem. Phys.* 2004, **6**, 2763-2771. (g) M. Z. Zgierski, S. Patchkovskii, T. Fujiwara, E. C. Lim, *J. Phys. Chem. A* 2005, **109**, 9384-9387. (h) L. Blancafort, *Photochem. Photobiol.* 2007, **83**, 603-610. (i) L. Blancafort, A. Migani, *J. Photochem. Photobiol. A* 2007, **190**, 283-289. (j) Q. Li, B. Mennucci, M. A. Robb, L. Blancafort, C. Curutchet, *J. Chem. Theory Comput.* 2015, **11**, 1674-1682.
- (7) (a) H. R. Hudock, T. Martínez, *ChemPhysChem* 2008, **9**, 2486-2490. (b) J. González-Vázquez, L. González, *ChemPhysChem* 2010, **11**, 3617-3624.
- (8) (a) K. A. Kistler, S. Matsika, *Phys. Chem. Chem. Phys.* 2010, **12**, 5024-5031. (b) K. A. Kistler, S. Matsika, *J. Phys. Chem. A* 2009, **113**, 12396-12403. (c) K. A. Kistler, S. Matsika, *J. Chem. Phys.* 2008, **128**, 215102. (d) K. A. Kistler, S. Matsika, *J. Phys. Chem. A* 2007, **111**, 8708-8716. (e) C. G. Triandafillou, S. Matsika, *J. Phys. Chem. A* 2013, **117**, 12165-12174.
- (9) (a) M. Barbatti, D. Nachtigallova, A. J. A. Aquino, J. J. Szymczak, P. Hobza, H. Lischka, *Proc. Natl. Acad. Sci. USA* 2010, **107**, 21453-21458. (b) M. Barbatti, A. J. A. Aquino, J. J. Szymczak, D. Nachtigallova, H. Lischka, *Phys. Chem. Chem. Phys.* 2011, **13**, 6145-6155.
- (10) (a) A. Nakayama, S. Yamazaki, T. Taketsugu, *J. Phys. Chem. A* 2014, **118**, 9429-9437. (b) A. Nakayama, Y. Harabuchi, S. Yamazaki, T. Taketsugu, *Phys. Chem.*

- Chem. Phys.* 2013, **15**, 12322–12339.
- (11) (a) S S. Lobsiger, M. A. Trachsel, H.-M. Frey, S. Leutwyler, *J. Phys. Chem. B* 2013, **117**, 6106–6115. (b) M. A. Trachsel, S. Lobsiger, S. Leutwyler, *J. Phys. Chem. B* 2012, **116**, 11081–11091.
- (12) (a) H. Y. Kang, K. T. Lee, B. Y. Jung, Y. J. Ko, S. K. Kim, *J. Am. Chem. Soc.* 2002, **124**, 12958-12959. (b) S. Ullrich, T. Schultz, M. Z. Zgierski, A. Stolow, *Phys. Chem. Chem. Phys.* 2004, **6**, 2796-2801. (c) C. Canuel, M. Mons, F. Piuuzzi, B. Tardivel, I. Dimicoli, M. Elhanine, *J. Chem. Phys.* 2005, **122**, 074316. (d) K. Kosma, C. Schroter, E. Samoylova, I. V. Hertel, T. Schultz, *J. Am. Chem. Soc.* 2009, **131**, 16939-16943.
- (13) (a) M. F. Denissenko, J. X. Chen, M. S. Tang, G. P. Pfeifer, *Proc. Natl. Acad. Sci. U.S.A.* 1997, **94**, 3893-3898. (b) Y.-H. You, P. E. Szabo, G. P. Pfeifer, *Carcinogenesis* 2000, **21**, 2113-2117. (c) G. P. Pfeifer, Y. H. You, A. Besaratinia, *Mutat. Res.* 2005, **571**, 19-31. (d) T. Douki, J. Cadet, *Biochem.* 2001, **40**, 2495-2501. (e) J. Cadet, P. Vigny, *The Photochemistry of Nucleic Acid In Bioorganic Photochemistry*; Morrison, H., Ed.; John Wiley & Sons: New York, 1990, 1-272. (f) J. Cadet, S. Mouret, J.-L. Ravanat, T. Douki, *Photochem. Photobiol.* 2012, **88**, 1048-1065.
- (14) (a) W.-M. Kwok, C. Ma, D. L. Phillips, *J. Am. Chem. Soc.* 2006, **128**, 11894-11905. (b) W.-M. Kwok, C. Ma, D. L. Phillips, *J. Am. Chem. Soc.* 2008, **130**, 5131-5139. (c) W.-M. Kwok, C. Ma, D. L. Phillips, *J. Phys. Chem. B* 2009, **113**, 11527-11534.
- (15) (a) C. T. L. Chan, C. C. W. Cheng, K. Y. F. Ho, W.-M. Kwok, *Phys. Chem. Chem. Phys.* 2011, **13**, 16306–16313. (b) C. Ma, C. T. L. Chan, W.-M. Kwok, C.-M. Che, *Chem. Sci.* 2012, **3**, 1883–1892. (c) C. Ma, W.-M. Kwok, W. S. Chan, P. Zuo, J. T. W. Kan, P. H. Toy, D. L. Phillips, *J. Am. Chem. Soc.* 2005, **127**, 1463-1427. (d) C. Ma, W.-M. Kwok, W. S. Chan, Y. Du, J. T. W. Kan, P. H. Toy, D. L. Phillips, *J. Am. Chem. Soc.* 2006, **128**, 2558-2570.
- (16) (a) L. Blancafort, B. Cohen, P. M. Hare, B. Kohler, M. A. Robb, *J. Phys. Chem. A* 2005, **109**, 4431-4436. (b) M. Daniels, W. Hauswirth, *Science* 1971, **171**, 675-677. (c) P. R. Callis, *Chem. Phys. Lett.* 1979, **61**, 563-567. (d) C. Párkányi, C. Boniface, J.-J. Aaron, M. D. Gaye, R. Ghosh, L. V. Szentpály, K. S. Raghuveer, *Structural Chemistry* 1992, **3**, 277-289.
- (17) (a) M. Merchán, L. Serrano-Andrés, M. A. Robb, L. Blancafort, *J. Am. Chem. Soc.* 2005, **127**, 1820-1825. (b) R. González-Luque, T. Climent, I. González-Ramírez, M. Merchán, L. Serrano-Andrés, *J. Chem. Theory Comput.* 2010, **6**, 2103–2114.
- (18) (a) H. Görner, *J. Photochem. Photobiol. B* 1990, **5**, 359-377. (b) I. G. Gut, P. D. Wood, R. W. Redmond, *J. Am. Chem. Soc.* 1996, **118**, 2366-2373. (c) P. D. Wood, R. W. Redmond, *J. Am. Chem. Soc.* 1996, **118**, 4256-4263. (d) Z.-H. Zuo, A.-D. Yao, J.

- Luo, W.-F. Wang, J.-S. Zhang, N.-Y. Lin, *J. Photochem. Photobiol. B: Biol* 1992, **15**, 215-222.
- (19) *Solvents and Solvent Effects in Organic Chemistry*, 4th ed., Reichardt, C., Welton, T., Eds., WILEY-VCH Verlag GmbH & Co. KGaA: Weinheim, 2011.
- (20) (a) R. Improta, V. Barone, *Theor. Chem. Acc.* 2008, **120**, 491–497. (b) R. So, S. Alavi, *J. Comput. Chem.* 2006, **28**, 1776–1782.
- (21) (a) C. L. Deasy, *Chem. Rev.* 1945, **36**, 145-155. (b) K.U. Ingold, G. A. Dilabio, *Org. Lett.* 2006, **8**, 5923–5925.
- (22) L. Esposito, A. Banyasz, T. Douki, M. Perron, D. Markovitsi, R. Improta, *J. Am. Chem. Soc.* 2014, **136**, 10838-10841.
- (23) (a) R. Jimenez, G. R. Fleming, P. V. Kumar and M. Maroncelli, *Nature*, 1994, **369**, 471. (b) M. L. Horng, J. A. Gardecki, A. Papazyan and M. Maroncelli, *J. Phys. Chem.* 1995, **99**, 17311-17337.
- (24) V. Karunakaran, K. Kleinermanns, R. Improta, S. A. Kovalenko, *J. Am. Chem. Soc.* 2009, **131**, 5839-5850.
- (25) (a) W. H. Gmeiner, C. D. Poulter, *J. Am. Chem. Soc.* 1988, **110**, 7640-7647. (b) M. M. E. Scheffers-Sap, H. M. Buck, *J. Am. Chem. Soc.* 1980, **102**, 6422-6424. (c) L. Katz, S. Penman, *J. Mol. Biol.* 1966, **15**, 220-231.